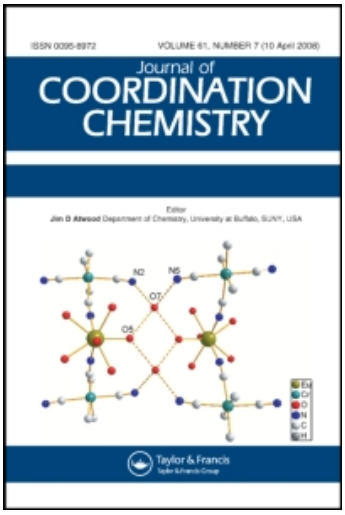

Journal of Coordination Chemistry
Publication details, including instructions for authors and subscription information:
http://www.informaworld.com/smpp/title~content=t713455674

Synthesis, characterization and biological activity of triaminoxime and its metal complexes

Winfried Plass[a]; Abdou Saad El-Tabl[b]; Axel Pohlmann[a]
[a] Chemistry Department, Friedrich-Schiller Universität, Jena, Germany [b] Faculty of Science, Chemistry Department, Menoufia University, Shebin El-Kom, Egypt

First published on: 10 December 2009

To cite this Article Plass, Winfried , El-Tabl, Abdou Saad and Pohlmann, Axel(2009) 'Synthesis, characterization and biological activity of triaminoxime and its metal complexes', Journal of Coordination Chemistry, 62: 3, 358 — 372, First published on: 10 December 2009 (iFirst)
To link to this Article: DOI: 10.1080/00958970802279790
URL: http://dx.doi.org/10.1080/00958970802279790

Journal of Coordination Chemistry
Vol. 62, No. 3, 10 February 2009, 358–372

Taylor & Francis
Taylor & Francis Group

Synthesis, characterization and biological activity of triaminoxime and its metal complexes

WINFRIED PLASS†, ABDOU SAAD EL-TABL*‡ and AXEL POHLMANN†

†Chemistry Department, Friedrich-Schiller Universität, Jena, Germany
‡Faculty of Science, Chemistry Department, Menoufia University, Shebin El-Kom, Egypt

(*Received 7 February 2008; in final form 30 April 2008*)

Mn(II), Fe(III), Co(II), Ni(II), Cu(II) and Zn(II) complexes of multifunctional triaminoxime have been synthesized and characterized by elemental analyses, IR, UV–Vis spectra, magnetic moments, ^{1}H- and ^{13}C-NMR spectra for ligand and its Ni(II) complex, mass spectra, molar conductances, thermal analyses (DTA, DTG and TG) and ESR measurements. The IR spectral data show that the ligand is bi-basic or tri-basic tetradentate towards the metals. Molar conductances in DMF indicate that the complexes are non-electrolytes. The ESR spectra of solid copper(II) complexes $[(HL)(Cu)_2(Cl)_2]\cdot 2H_2O$ (**2**) and $[(L)(Cu)_3(OH)_3(H_2O)_6]\cdot 7H_2O$ (**6**) show axial symmetry of a $d_{x^2-y^2}$ ground state; however, [(HL)(Co)] (**4**) shows an axial type with d_{Z^2} ground state and manganese(II) complex $[(L)(Mn)_3(OH)_3(H_2O)6]\cdot 4H_2O$ (**10**) shows an isotropic type. The biological activity of the ligand and its metal complexes are discussed.

Keywords: Complexes; Synthesis; Spectral and magnetic studies

1. Introduction

Development of more effective antifungal and antibiotic compounds is required for resistance of bacterial infections arising from depressed immune system, as in chemotherapy, the use of drugs to avoid organ rejection in transplanted patients and diseases like AIDS [1, 2]. Growing interest in triazine and aminoguanidine derivatives stems from their potential application as agrochemicals and applications in the fields of optics, herbicides and pharmaceuticals; recent studies have shown their ability in chelating transition metal ions to form stable metal complexes [3–8]. Guaidinopropionic acid has been demonstrated to improve insulin sensitivity and to promote weight loss selectively from adipose tissue in animal models of non-insulin dependent diabetes mellitus [9]. Oximes and their metal complexes have applications in many important chemical processes in the areas of medicine, bioorganic systems, catalysis, electrochemical and electro optical sensors [10–13]. Metal complexes of oxime ligands have been examined as compounds with columnar stacking, which is thought to be the reason for their semiconducting properties [10], and as model compounds which mimic bio-functions such as the reduction of vitamin B_{12} [11].

*Corresponding author. Email: asaeltabl@yahoo.com

Journal of Coordination Chemistry
ISSN 0095-8972 print/ISSN 1029-0389 online © 2009 Taylor & Francis
DOI: 10.1080/00958970802279790

Most of the work reported on triaminoguidine Schiff bases has centered around those derived from simple aldehydes and ketones [5, 14]. The limited information available on metal complexes of aminoguidine oxime Schiff bases prompted us to undertake systematic research in this field. In the present work, Mn(II), Fe(III), Ni(II), Co(II), Cu(II) and Zn(II) complexes of triaminoguidine oxime are prepared and characterized by elemental and spectroscopic analyses.

2. Experimental

Reagent grade chemicals were used. Diacetylmonoxime [14] and triaminoguanidinum chloride [15] were prepared by literature methods. Carbon, hydrogen, nitrogen and chlorine were determined at the Institute für Organische and Makromolekulare Chemie, Friedrich-Schiller University, Jena, Germany, using LECO CHN/932 and VARIOEIII elemental analyzers. Standard methods [for Ni(II), Fe(III) and Co(II) ions (gravimetric method), Cu(II) ion (EDTA titration) and Zn(II) ion (thermogravimetric method] were used to determine the metal ion content [16]. All metal complexes were dried in air. The IR spectra were recorded on a Bruker IFS 55/Equinox spectrometer on compounds prepared as KBr pellets. Electronic spectra were recorded on a Varian Cary 5000 UV/VIS/NIR spectrophotometer as nujol mull and MeOH (qualitative). The conductances of 10^{-3} M solutions of the complexes in DMF were measured at 25°C with a Bibby conductimeter type MCI. The magnetic susceptibilities of the complexes were measured with a SQUID susceptometer MPM 55 on polycrystalline samples at a field of 1000 Oe. ^{1}H- and ^{13}C-NMR spectra were recorded on Bruker Avance 200 and 400 MHZ spectrometers. Mass spectrometry was conducted on a Mat 95 × L Finnegan instrument using electron spray ionization, negative and positive mode. Thermal analyses were carried out using a NETZSCHSTA 409Pc/PG instrument. The samples were placed in a heating block with a heating rate of 5 K/min under nitrogen. All ESR measurements on solid complexes at 300 K and 77 K were made using a Bruker ESR 300 E, using *x*-band (9 GHZ). DppH was used as a standard.

2.1. *Preparation of the ligand and its metal complexes*

2.1.1. Ligand [H_3L] (1). It was prepared analogous to procedures reported in the literature [5, 17].

2.1.2. Complexes 2, 3, 4 and 5. They were prepared by mixing stoichiometric ratios (1:1 or 1:2) of the ligand (0.01 mol, 5.0 g) (30 mL EtOH) with the appropriate metal chloride in 35 mL EtOH. For (**2**) $CuCl_2 \cdot 2H_2O$ (0.01 mol, 1.95 g) or (0.02 mol, 3.9 g), complexes (**3**) $NiCl_2 \cdot 6H_2O$ and (**4**) $CoCl_2 \cdot 6H_2O$ (0.01 mol, 2.71 g) or (0.02 mol, 5.42 g) and for (**5**) $FeCl_3 \cdot 6H_2O$ (0.01 mol, 3.1 g) or (0.02 mol, 6.19 g). Five drops of piperidine were added to the mixture and the mixture was refluxed for 2 h. On cooling to room temperature, fine crystals which formed were filtered off, washed several times with EtOH and dried in air.

2.1.3. Complexes 6, 7, 8, 9 and 10. They were prepared by mixing stoichiometric ratio (1 : 3) of the ligand (0.01 mol, 5.0 g) (30 mL EtOH) with the appropriate metal acetate in 50 mL EtOH. For (**6**) $Cu(OAc)_2 \cdot H_2O$ (0.03 mol, 6.85 g), complexes (**7**) $Ni(OAc)_2 \cdot 4H_2O$ and (**8**) $Co(OAc)_2 \cdot 4H_2O$ (0.03 mol, 8.51 g), (**9**) $Zn(OAc)_2 \cdot 2H_2O$ (0.03 mol, 7.45 g) and (**10**) $Mn(OAc)_2 \cdot 4H_2O$ (0.03 mol, 8.34 g). Three moles of KOH (0.03 mol, 1.92 g) in 15 mL H_2O were added to the mixture. The mixture was heated at reflux with stirring for three hours. On cooling to room temperature, fine crystals were filtered off, washed several times with EtOH and subsequently dried in air.

2.2. *Microbiology*

Fungus media. Czapek Dox agar medium was prepared (g L^{-1} distilled water) 1 gm yeast extract, (30 g) sucrose, (2 g) $NaNO_3$, (15 g) agar, (0.5 g) KCl, (1 g L^{-1}) KH_2PO_4, (0.5 g) $MgSO_4 \cdot 7H_2O$ and a trace of $FeCl_3 \cdot 6H_2O$. The pH was adjusted to 5.5 by (NaOH, HCl) and this medium was then sterilized by autoclaving at 120°C for 15 min. After cooling to 45°C, the medium was poured into 90 mm diameter Petri dishes (approx. 20 mL each) and incubated at 37°C. After a few hours, the Petri dishes were stored at 4°C and *Aspergillus niger* was spread over each dish by using sterile bent Loop rod. Disks were cut by a sterilized cork borer and then taken by sterilized needle. The resulting pits are sites for the tested compounds. The plates are incubated at 30°C for 24–48 h and then any clear zones present were detected.

3. Results and discussion

The reaction of triaminoguidine with diacetylmonoxime in EtOH, 1 : 3 molar ratio, led to the formation of ligand $[H_3L]$ (**1**), as shown in scheme 1.

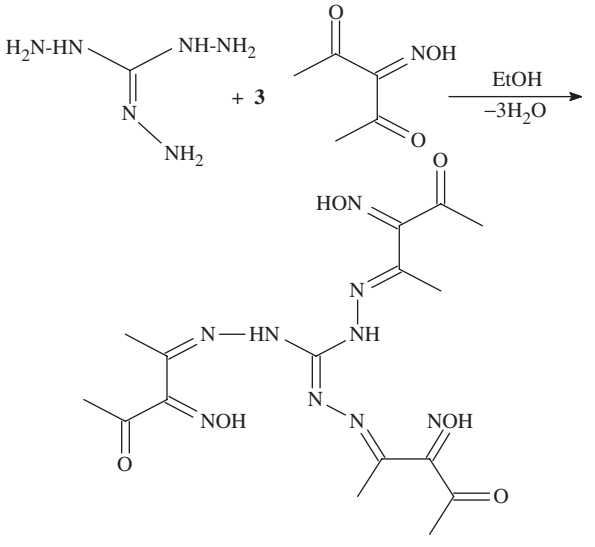

Scheme 1. The preparation of the ligand.

Reaction of **1** with metal ions in the presence of piperidine or KOH gives **2**–**10** with different geometries. All the prepared compounds are colored, non hygroscopic, crystalline solids, stable at room temperature. The complexes are insoluble in nonpolar and polar solvents but soluble in polar coordinating solvents such as DMSO and DMF. Elemental analyses, physical data (table 1) and spectral data (tables 2 and 3), are compatible with the proposed structures, as shown in figure 1. To date, no diffraction quality crystals have been grown.

3.1. *^{1}H- and ^{13}C-NMR spectra*

The ^{1}H-NMR spectra of **1** and its nickel(II) complex in deuterated DMSO show signals consistent with the proposed structure. For **1**, the peaks in the 7.12–7.44 ppm range are assigned to protons of NH group [18, 19]. The signal of >C=NOH is at 12.98 ppm [20]. Resonances at 3.29–3.76 and 2.21–3.0 ppm are due to acetyl and methyl groups, respectively [18, 21]. The ^{13}C-NMR spectrum of **1** in deuterated DMSO shows peaks at 200.13, 194.86, 156.29 and 56.00 ppm corresponding to acetyl, oxime and imino groups, respectively [18, 21, 22], and peaks at 38.88–40.13 ppm are assigned to the methyl group [18]. The ^{1}H-NMR spectrum of **3** shows chemical shift of =NOH at 11.1 ppm and the singlet observed at 7.0 ppm is due to NH. The signals in the 2.3–1.9 ppm range are assigned to acetyl and methyl protons.

3.2. *Conductivity measurements*

The molar conductance values of the complexes in DMF (10^{-3} M) lie in the 2.3–33 $\Omega\,mol^{-1}\,cm^{2}$ range (table 1), indicating that all the complexes are not electrolytes [23, 24]. This confirms that the anion is coordinated to the metal ion.

3.3. *IR spectra*

The mode of bonding between the ligand and the metal can be revealed by comparing the IR spectra of the solid complexes with that of the ligand. The IR spectral data for the ligand and its metal complexes are presented in table 2. The IR spectrum of **1** shows broad, medium bands in the 3500–2900 and 2850–2500 cm^{-1} ranges, attributed to intra- and intermolecular hydrogen bonds between >C=NOH and >C=N or >C=O groups [18, 25]. Thus, the higher frequency band is associated with a weaker hydrogen bond and the lower frequency band with a stronger hydrogen bond. The spectrum also shows bands at 3476 and 3446, 3150 and 3100 cm^{-1}, assigned to ν(OH) and ν(NH), respectively [20, 26]. Bands at 1684, 1617 and 1560 cm^{-1} correspond to ν(C=O), ν(C=N) and ν(N–O), respectively [27, 28]. Medium bands at 1090 and 995 cm^{-1} are assigned to ν(N–O) [20, 29]. Complexes **2**, **3** and **4** show a broad band in the 3580–2990 cm^{-1} range (table 2) due to intramolecular hydrogen bond between –NOH with imine group; however, **5** shows a band at 3520–2820 cm^{-1}, attributed to hydrogen bond of NOH with chloride [25]. Complexes **2**, **3** and **5** show a broad band in the 3530–3100 cm^{-1} range, assigned to hydrated or coordinated water molecules (table 2). Complexes **6**–**10** show a broad band in the 3460–2850 cm^{-1} range due to hydrogen bonding and hydrated water in the 3520–3000 cm^{-1} range. Complexes **6** and **10** show

Table 1. Elemental analyses and physical properties of H_3L and its metal complexes.

Comp. No.	Molecular formula	M. wt.	Color	Yield (%)	M.P. (°C)	$\Omega\,mol^{-1}\,cm^2$	μ_{eff} (B.M.)	Found (Calcd %) C	H	N	M	Cl
1	$[H_3L]$		Pale brown	78.0	>300	–	–	43.92	5.69	28.1	–	–
	$[C_{16}H_{23}N_9O_6]$	437.34						(43.93)	(5.26)	(28.83)	–	–
2	$[(HL)(Cu)_2(Cl)_2]\cdot 2H_2O$		Brown	68.3	>300	8.62	1.52	28.25	3.48	19.03	18.23	10.11
	$[C_{16}H_{25}N_9O_8Cl_2Cu_2]$	669.36						(28.7)	(3.74)	(18.83)	(18.98)	(10.61)
3	$[(HL)(Ni)]\cdot 2H_2O$		Reddish	75.6	>300	2.31	Diam.	36.54	4.9	23.82	10.9	–
	$[C_{16}H_{25}N_9O_8Ni]$	529.38	brown					(36.23)	(4.72)	(23.7)	(11.3)	–
4	$[(HL)(Co)]$		Deep	75.2	>300	2.53	1.88	39.67	4.8	25.66	11.25	–
	$[C_{16}H_{21}N_9O_6Co]$	493.33	brown					(38.94)	(4.25)	(25.55)	(11.76)	–
5	$[(HL)(Fe)_2(Cl)_4(H_2O)]\cdot 6H_2O$		Brown	58.5	>300	11.12	1.73	23.67	4.21	14.83	12.98	16.56
	$[C_{16}H_{37}N_9O_{14}Cl_4Fe_2]$	834.46						(23.26)	(4.43)	(15.11)	(13.43)	(17.03)
6	$[(L)(Cu)_3(OH)_3(H_2O)_6]\cdot 7H_2O$		Greenish	80.1	>300	3.82	1.84	20.67	5.3	13.72	20.34	–
	$[C_{16}H_{49}N_9O_{22}Cu_3]$	910.55	brown					(21.1)	(5.4)	(13.84)	(20.99)	–
7	$[(L)(Ni)_3(OH)_3]\cdot H_2O$		Yellowish	85.0	>300	33.10	Diam.	27.82	4.1	19.11	25.83	–
	$[C_{16}H_{25}N_9O_{10}Ni_3]$	677.36	golden					(28.36)	(3.69)	(18.61)	(25.7)	–
8	$[(L)(Co)_3(OH)_3]\cdot 4H_2O$		Brown	75.4	>300	4.32	4.12	26.48	4.4	17.0	24.23	–
	$[C_{16}H_{31}O_{13}N_9Co_3]$	731.4						(26.26)	(4.24)	(17.23)	(23.8)	–
9	$[(L)(Zn)_3(OH)_3]\cdot 5H_2O$		Yellowish	78.1	>300	2.71	Diam.	24.73	3.7	16.21	24.97	–
	$[C_{16}H_{33}N_9O_{14}Zn_3]$	770.42	brown					(24.93)	(4.28)	(16.36)	(25.32)	–
10	$[(L)(Mn)_3(OH)_3(H_2O)_6]\cdot 4H_2O$		Deep	67.3	>300	7.13	5.96	22.98	5.02	14.86	19.23	–
	$[C_{16}H_{43}N_9O_{19}Mn_3]$	830.5	brown					(23.13)	(5.18)	(15.2)	(19.88)	–

Table 2. IR spectra (assignments) of H_3L and its metal complexes.

	Assignments (cm^{-1})								
Comp. No.	ν(NOH/OH)	ν(H_2O+H=bond)	ν(NH)	ν(C=O)	$\nu(C=N)_{imine}$	$\nu(C=N)_{oxime/triamino}$	ν(NO/NOH)	ν(MO)	ν(MN)
1	3476, 3446	3500–2900 2850–2500	3150, 3100	1684	1617 1560	1588 1560	1090, 995	–	–
2	3435	3560–3050 3530–3200	3200	1701 1654	1615	1580 1558	1165 1016, 895	660	616
3	3420	3580–2990 3510–3150	3225, 3185	1705 1670	1612	1575 1555	1196 1021, 926	–	585
4	3450	3550–3000	3213, 3180	1715 1668	1610	1568 1559	1193 1011, 947	–	618
5	3420	3530–2850 3500–3100	3225	1642	1611	1565 1550	1175 1026, 980	667	587
6	3365	3520–3200 3180–2780 3380–2980	3270	1670	1610	1570 1540	1160	618	530
7	3300	3520–3150 3430–2910	3240, 3185	1670	1612	1575 1538	1180	585	485
8	3350	3500–3000 3350–2950	3260	1665	1615	1568 1542	1160	672	617
9	3315	3510–3170 3460–3000	3250	1656	1610	1590 1535	1200	668	618
10	3250	3500–3170 3150–2950 3420–2850	3250	1654	1608	1565 1540	1185	668	560

Table 3. Electronic spectra of the ligand (H_3L) and its metal complexes.

Complex No.	Medium	λ (nm)	Transition assignment
1	N.M.	325, 300	
	MeOH	310 nm ($\varepsilon = 0.2 \times 10^{-2}$ mol^{-1} cm^{-1})	$n \rightarrow \pi^*$
		285 nm ($\varepsilon = 0.22 \times 10^{-2}$ mol^{-1} cm^{-1})	$\pi \rightarrow \pi^*$
2	N.M.	590, 530, 410,325, 308, 255	$^2B_{1g} \rightarrow {}^2A_{1g}$, $^2B_{1g} \rightarrow {}^2E_g$, $^2B_{1g} \rightarrow {}^2B_{2g}$, Cl $\rightarrow$ Cu charge transfer
	MeOH	525, 485, 250	$n \rightarrow \pi^*$, $\pi \rightarrow \pi^*$
3	N.M.	540, 425, 300, 265	$^3T_1 \rightarrow {}^3T_2$, $^3T_1(F) \rightarrow {}^3T_2(P)$
	MeOH	520, 415, 260	$n \rightarrow \pi^*$, $\pi \rightarrow \pi^*$
4	N.M.	530, 435, 380, 298, 260	$^1A_{1g} \rightarrow {}^1B_{1g}$
	MeOH	510, 415, 255	$n \rightarrow \pi^*$, $\pi \rightarrow \pi^*$
5	N.M.	635, 430, 350, 295, 266	$^6A_1 \rightarrow {}^4T_1$, charge transfer
	MeOH	620, 410, 370, 260	$n \rightarrow \pi^*$, $\pi \rightarrow \pi^*$
6	N.M.	624, 560, 445, 305, 265	$^2B_1 \rightarrow {}^2B_2$, $^2B_1 \rightarrow {}^2E$, ligand $\rightarrow$ copper charge transfer
	MeOH	610, 515, 410, 260	$n \rightarrow \pi^*$, $\pi \rightarrow \pi^*$
7	N.M.	515, 435, 305, 260	$^3T_1 \rightarrow {}^3T_2$, $^3T_1(F) \rightarrow {}^3T_2(P)$
	MeOH	505, 410, 250	$n \rightarrow \pi^*$, $\pi \rightarrow \pi^*$
8	N.M.	550, 450, 362, 298, 260	$^1A_{1g} \rightarrow {}^1B_{1g}$
	MeOH	525, 420, 250	$n \rightarrow \pi^*$, $\pi \rightarrow \pi^*$
9	N.M.	370, 300, 268	$n \rightarrow \pi^*$, $\pi \rightarrow \pi^*$
	MeOH	350, 275, 250	
10	N.M.	660, 575, 345, 295, 265	$^6A_1 \rightarrow {}^4T_{1g}$, $^6A_1 \rightarrow {}^4T_{2g}$, $^6A_1 \rightarrow {}^4E_g$,
	MeOH	645, 510, 340, 255	$n \rightarrow \pi^*$, $\pi \rightarrow \pi^*$

N.M. = Nujol mull.

additional bands in the 3180–2780 cm^{-1} range, attributed to coordinated water molecules (table 2) [18, 30, 31]. Complexes **2**, **3**, **4** and **5** show a band at 3450–3420 cm^{-1} range due to $\nu(OH)_{oxime}$; however, complexes **6**–**10** show a band at 3365–3250 cm^{-1} range corresponding to $\nu(OH)_{coord}$ [25, 32]. The ν(NH) appears in the 3270–3185 cm^{-1} range [18, 33]. The complexes show a band at 1715–1642 cm^{-1} (table 2), which corresponds to ν(C=O) [18, 33, 34] and bands appearing in the 1615–1608 and 1590–1565 cm^{-1} ranges due to $\nu(C{=}N)_{imine}$ and $\nu(C{=}N)_{oxime}$, respectively [18, 20]. Complexes **2**–**5** show ν(NOH) at 1026–1011 and 980–926 cm^{-1} ranges (table 2) [20, 32]. The complexes show ν(NO) band at 1200–1160 cm^{-1} range, indicating N-coordinated oximato group [25]. Complexes **2** and **5** show bands at 365 and 385 cm^{-1}, respectively, indicating ν(M–Cl) [18, 25]. The bonding of the metal ions to the ligand through the oxygen and nitrogen atoms is further supported by the presence of new bands in the 672–618 and 618–485 cm^{-1} ranges due to ν(M–O) and ν(M–N), respectively [18, 35–37].

3.4. *Electronic spectra*

The significant electronic absorption bands of the ligand and metal complexes are presented in table 3. In nujol mull, the ligand shows bands at 325 and 300 nm, however, in methanol the bands are at 285 nm ($\varepsilon = 0.22 \times 10^{-2}$ mol^{-1} cm^{-1}) and 310 nm ($\varepsilon = 0.2 \times 10^{-2}$ mol^{-1} cm^{-1}). These bands are assigned to $\pi \rightarrow \pi^*$ and $n \rightarrow \rightarrow \pi^*$ transitions, respectively [38, 39]. In metal complexes, the charge transfer bands are

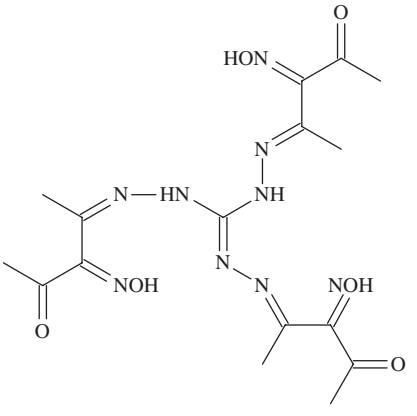

[H_3L], (**1**)

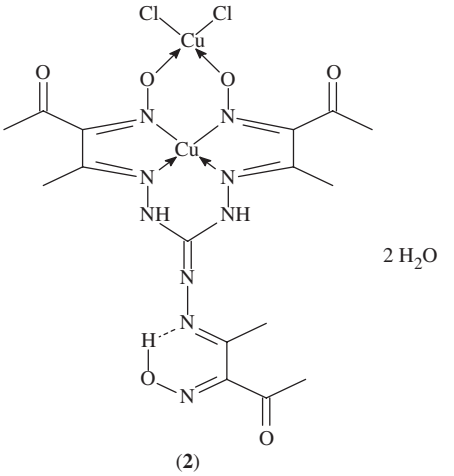

(**2**)

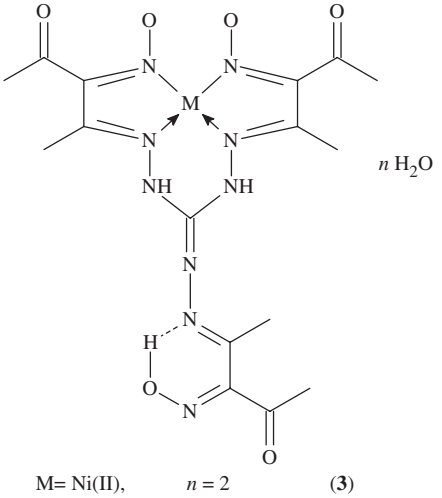

M= Ni(II), $n = 2$ (**3**)
M = Co(II), $n = 0$ (**4**)

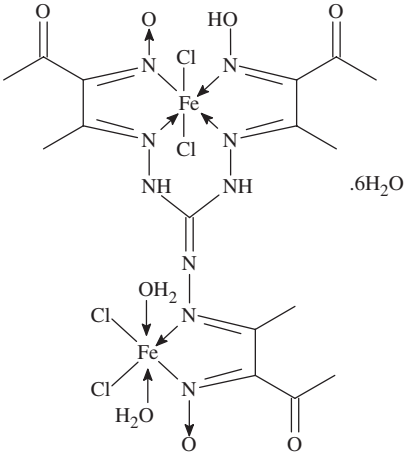

(**5**)

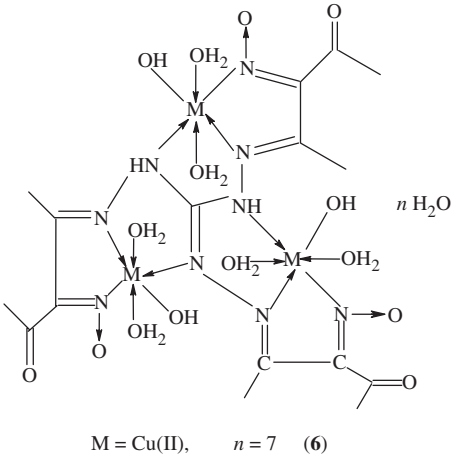

M = Cu(II), $n = 7$ (**6**)
M = Mn(II), $n = 4$ (**10**)

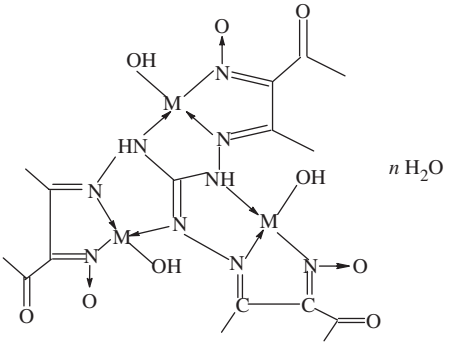

M = NI(II), $n = 1$ (**7**)
M = Co(II), $n = 4$ (**8**)
M = Zn(II), $n = 5$ (**9**)

Figure 1. Structural representation of the complexes.

observed, in nujol mull at 370–255 nm and in methanol, at 350–250 nm ranges. The shift of bands to relatively higher or lower energies with their broadness can be explained due to N → M LMCT transition and deprotonation. The nickel(II) complexes **3** and **7** show bands (table 3) indicating square planar environment around the nickel(II); absence of any band below 900 nm rules out the possibility of tetrahedral structure for the nickel chelate [40, 41]. The cobalt(II) complexes **4** and **8** show bands (table 3) which are similar to square planar cobalt(II) complexes [23, 42–44]. The copper(II) complexes **2** and **6** show different bands. For complex **2**, the bands correspond to a square planar geometry [44, 45], however, in **6** the bands are assigned to a distorted octahedral structure [44, 46]. Iron(III) complex **5** shows bands (table 3) suggesting distorted octahedral geometry around iron(III) [18, 44, 47]. Manganese(II) complex **10** shows bands (table 3) which are compatible to an octahedral geometry around manganese(II) [18, 44, 48]. Zinc(II) complex **9** shows bands (table 3) indicating intraligand transitions. The broadness of the bands observed can be taken as an indication of distortion from perfect symmetry.

3.5. *Magnetic moments*

The magnetic moments of the metal complexes **2**–**10** at room temperature are shown in table 1. Nickel(II) complexes **3** and **7** are diamagnetic, indicating a square planar geometry around nickel(II) [23]. Cobalt(II) complexes **4** and **8** show values 1.88 and 4.12 B.M., respectively, indicating square planar geometry around cobalt(II) in low and high spin states [49–51]. The copper(II) complexes **2** and **6** show values 1.52 and 1.84 B.M., the value of complex **2** is below the spin-only value (1.73 B.M.), indicating spin-exchange interactions take place through the oxygen atom of the oximato group between the copper(II) ions in a square planar geometry [25, 50, 52]; however, the moment of complex **6** corresponds to one unpaired electron in an octahedral structure [53, 54]. Complex **5** has a value 1.73 B.M., indicating low spin iron(III) complex in an octahedral structure [42]. However, complex **10** shows a value 5.96 B.M., suggesting a high spin state in an octahedral structure [18, 55]. Zinc(II) complex **9** is diamagnetic as expected for a d^{10} configuration.

3.6. *ESR spectra*

The ESR spectra of the solid copper(II) complexes **2** and **6** at room and liquid nitrogen temperatures are characteristic of a d^9 system with axial symmetry and a $d_{x^2-y^2}$ ground state, common for copper(II) complexes [50, 56, 57]. On lowering the temperature to liquid nitrogen, the spectra are not changed, indicating that the geometry of the complexes are not changed on cooling. The *g*-values suggest square planar **2** and an octahedral **6**. The complexes show $g_\parallel > g_\perp > g_e$, confirming square planar or distorted octahedral geometry around the copper(II) ion [58, 59]. The ESR parameters for **2** are $g_\parallel = 2.33$, $g_\perp = 2.09$ and $g_{iso} = 2.17$, $A_\parallel = 175\,G$, $A_\perp = 47.5\,G$ and $A_{iso} = 90\,G$, $G = 3.6$, $g_\parallel/A_\parallel = 131.6\,cm^{-1}$, $\alpha^2 = 1.0$, ${K_\perp}^2 = 0.96$ $K_\parallel^2 = 1.2$, $K^2 = 1.04$ and $K = 1.02$, $B^2 = 1.04$, $B_1^2 = 1.2$, $2B = -197.6$ and $a_d^2 = 84.12\%$, and for **6** they are $g_\parallel = 2.29$, $g_\perp = 2.06$ and $g_{iso} = 2.13$, $A_\parallel = 150\,G$, $A_\perp = 15\,G$ and $A_{iso} = 60\,G$, $G = 4.8$, $g_\parallel/A_\parallel = 143\,cm^{-1}$, $\alpha^2 = 0.68$, $K_\perp^2 = 0.78$, $K_\parallel^2 = 0.77$ $K^2 = 0.7$ and $K = 0.88$, $B^2 = 1.015$, $B_1^2 = 1.13$, $2B = -176.5$ and $a_d^2 = 75.1\%$, respectively. The *g*-values are related by the expression [60],

$G = (g_{\parallel} - 2)/(g_{\perp} - 2)$, if $G > 4.0$. When local tetragonal axes are aligned parallel or only slightly misaligned, if $G < 4.0$, significant exchange coupling is present. Complex **2** shows a value less than 4.0 (3.6), indicating spin-exchange interactions take place between copper(II) ions through oximato oxygen atoms (figure 1). This is confirmed from the magnetic moment value (table 1). However, **6** shows a value greater than 4.0 (4.8), indicating the presence of tetragonal axes in this complex, in agreement with the magnetic value (1.84). For $g_{\parallel}/A_{\parallel}$, the range reported for square planar complexes is 105 to 135 cm^{-1} and for tetragonal distorted complexes >135–250 cm^{-1} [54, 61], the $g_{\parallel}/A_{\parallel}$ value for **2** is 131.6 cm^{-1}, just within the range expected for square planar complexes, however, **6** is 143 cm^{-1}, indicating a distorted octahedral complex. Kivelson and Neiman [62] show that the $g_{\parallel}$-value in the copper(II) complexes can be used as a measure of covalent character of the metal-ligand bond. If this value is greater than 2.3, the environment is essentially ionic and the value less than this limit indicates a covalent environment, the $g_{\parallel}$-value for **2** is 2.33, indicating ionic character, however, **6** shows a value 2.29, indicating considerable covalent character [63–65]. The isotropic value of the hyperfine coupling constant (A_{iso}) is related to the σ-bonding parameter (α^2), through the following equation:

$$\alpha^2 = A_{iso}/PK + (g_{iso} - 2.0023)/K \tag{1}$$

where P is the free ion dipole term and K is the Fermi contact term occurring in the equation for the magnetic parameters given by McGarvery. If $\alpha^2 = 1$, the bond would be completely ionic, and if $\alpha^2 = 0.5$, the bond would be completely covalent, the calculated value for complex **2** is 1.0 indicating ionic bond character, however, complex **6** the value is 0.68 suggesting covalent bonding character [66]. The g-value of copper(II) complexes with a B_{1g}^2 ground state ($g_{\parallel} > g_1$) may be expressed by [66, 67]

$$g_{\parallel} = 2.002 - (8K_{\parallel}\lambda^{\circ}/\Delta E_{xy}) \tag{2}$$

$$g_{\perp} = 2.002 - (2K_{\perp}^2\lambda^{\circ}/\Delta E_{xz}) \tag{3}$$

where $K_{\parallel}$ and $K_{\perp}$ are the parallel and perpendicular components of the orbital reduction factor (K), λ°, is the spin-orbit coupling constant for the free copper, ΔE_{xy} and ΔE_{xz} are the electron transition energies. From the above relations, the orbital reduction of covalence [67] can be calculated; for an ionic environmental, $K = 1$ and for a covalent environmental $K < 1$, the lower the value of K, the greater the covalent character. By rearrangement of the above equations,

$$K_{\perp}^2 = (g_{\perp} - 2.002)\Delta E_{xz}/2\lambda^{\circ} \tag{4}$$

$$K_{\parallel}^2 = (g_{\parallel} - 2.002)\Delta E_{xy}/8\lambda^{\circ} \tag{5}$$

$$K^2 = (K_{\parallel}^2 + 2K_{\perp}^2)/3 \tag{6}$$

K-values of complexes **2** and **6** are 1.02 and 0.88, confirming the ionic and covalent bond characters [68, 69]. The in-plane and out-of plane π-bonding

coefficients (B_1^2 and B^2) are dependent upon the values of ΔE_{xz} and ΔE_{xy} in the following equation [65].

$$\alpha^2 B^2 = (g_\perp - 2.002)\Delta E_{xz}/2\lambda^\circ \quad (7)$$

$$\alpha^2 B_1^2 = (g_\parallel - 2.002)\Delta E_{xz}/8\lambda^\circ \quad (8)$$

The copper(II) complexes **2** and **6** show $B_1^2 = 1.2$ and 1.13 and $B^2 = 1.04$ and 1.015, respectively, indicating ionic bond character in the in-plane and out-of-plane π bondings [69, 70].

It is possible to calculate approximate orbital populations for d orbitals using the following equations

$$A_\parallel = A_{iso} - 2B[1 \pm (7/4)\Delta g_\parallel] \quad (9)$$

$$a_d^2 = 2B/2B^\circ \quad (10)$$

where $2B^\circ$ is the calculated dipolar couplings for unit occupancy of a d orbital. When the data are analyzed using the Cu^{63} hyperfine coupling and considering all the sign combinations, the only physically meaningful results are found when $A_\parallel$ and A are negative. The resulting isotropic coupling constants (A_{iso}) are −90 and −60G and the parallel components of the dipolar coupling (2B) are also negative, 1976 and −176.5G, respectively. The orbital populations for **2** and **6** are 84% and 75%, respectively, indicating a $d_{x^2-y^2}$ ground state [18, 54, 55, 70]. The ESR spectrum of cobalt(II) complex **4** shows $g_\perp > g_\parallel > 2.003$, indicating that the unpaired electron is present in dz^2 in a square planar environment [50, 58]. The ESR parameters are $g_\parallel = 2.06$, $g_\perp = 2.22$ and $g_{iso} = 2.17$, $A_\parallel = 90$ G, $A_\perp = 10$ G and $A_{iso} = 36.7$ G. These parameters are identical to square planar cobalt(II) complexes in low spin state [50, 65, 70]. However, **8** shows an axial spectrum with $g_\parallel > g_\perp > 2.0023$, indicating a square planar complex in a high spin state [65, 68, 70]. The ESR parameters are $g_\parallel = 2.28$, $g_\perp = 2.06$ and $g_{iso} = 2.13$, $A_\parallel = 130$ G, $A_\perp = 20$ G and $A_{sio} = 56.7$ G. The ESR spectrum of iron(III) complex **5** shows an isotropic type with $g_{iso} = 2.0032$, indicating an octahedral iron(III) complex in low spin state [50, 65, 68, 70], however, complex **10** shows an isotropic spectrum with $g_{iso} = 2.016$, indicating an octahedral geometry around manganese(II) in a high spin state [18, 50, 65, 70].

3.7. *ESI–MS studies*

The metal complexes have been investigated by ESI mass spectral analysis and the fragmentation data are consistent with the proposed structures (figure 1). The observation of the molecular ion allows an unambiguous identification, the most intense m/z peaks of the complexes are provided in Supplementary Material. ESI mass spectra of the complexes were recorded in 1 : 1 solvent mixture of MeOH and DMF because of solubility problems. The positive ion ESI masses observed for **2** show $[C_{10}H_{13}N_7O_3Cl_2Cu]^+$ (413.5, 100) and $[C_{16}H_{20}N_9O_6Cl_2Cu_2]^+$ (632, 15). Complex **3** shows $[C_8H_{16}N_8O_2]^+$ (256, 100) and $[C_{16}H_{24}N_9O_8Ni]^+$ (529, 10); **4** shows $[C_5H_6N_2O_2]$ (126,100) and $[C_{16}H_{20}N_9O_6Co]^+$ (493, 16); **5** shows $[C_5H_9N_6O]^+$ (169, 100) and $[C_{16}H_{19}N_9O_6ClFe_2]^+$ (581, 79); $[C_5H_7N_5O_2]^+$ (169, 76) and $[C_{16}H_{22}N_9O_9Cu_3]^+$ were observed for **6**; **8** and **9** show $[C_\parallel H1_{16}N_8O_6Co_3]^+$ (547, 100) and $[C_{16}H_{20}N_9O_6Co_3]^+$

(610, 60) and $[C_{13}H_{14}N_8O_6Zn_3]^+$ (573, 100) and $[C_{16}H_{20}N_9O_6Zn_3]^+$ (629, 10); **10** shows $[C_{10}H_{14}N_9O_3]^+$ (308, 60) and $[C_{16}H_{22}N_9O_9Mn_3]^+$ (649, 10).

3.8. *Thermal analyses*

Since the IR spectra of the metal complexes indicate the presence of water, thermal analyses (DTA, DTG and TG) were carried out to ascertain their nature. The DTA, DTG and TG curves in the temperature range 27–1000°C for the complexes show that the complexes are thermally stable to 60°C. Dehydration is characterized by an endothermic peak within 75–125°C, corresponding to loss of hydrated water [70, 71]. Complex **2** shows an endothermic peak at 89°C, with 5.77% weight loss (Calcd 5.38%) due to loss of $2H_2O$. Another endothermic peak was observed at 275°C with 11.54% weight loss (Calcd 11.22%), corresponding to loss of 2Cl atom. Exothermic peaks appeared at 350–650°C with 14.61% weight loss (Calcd 14.14%) due to the formation of CuO. Complex **3** showed an endothermic peak at 95–115°C with 7.2% weight loss (Calcd 6.8%) due to loss of $2H_2O$. The exothermic peak observed at 170°C with no weight loss could be due to breaking of hydrogen bonds; other exothermic peaks at 420–470°C, with 20.0% weight loss (Calcd 20.66%), correspond to formation of NiO [69–71]. Complex **4** showed endothermic peaks at 90–130°C with 12.85% weight loss (Calcd 12.95%), from loss of $C_4H_6O_2$ species. Another exothermic peak at 200°C with no weight loss could be due to loss of hydrogen bonding. The exothermic peak at 280°C with 10.29% weight loss (Calcd 10.54%) is assigned to loss of $C_3H_4ON_2$ and the exothermic peak at 495°C corresponds to formation of CoO. Complex **5** has an endothermic peak at 85°C with 12.62% weight loss (Calcd 12.96) due to loss of $6H_2O$, endothermic peak at 200°C, with 4.84% weight loss (Calcd 4.96%), assigned to the loss of coordinated water ($2H_2O$); two exothermic peaks at 280°C and 380°C, with 20.96% weight loss (Calcd 20.61%), correspond to loss of chlorine (4Cl); an exothermic peak at 450°C, with 13.0% weight loss (Calcd 13.16%), assigned to formation of FeO. Complex **6** showed an endothermic peak at 75–125°C with 13.56% weight loss (Calcd 13.84%) due to loss of $7H_2O$; an endothermic peak at 200°C, with 20.58% weight loss (Calcd 20.28%), assigned to loss of coordinated water ($6H_2O$) and hydroxide (3OH); exothermic peaks at 260 and 480°C, with 22.28% and 16.13% weight losses (Calcd 22.59 and 16.42%), corresponding to loss of $C_5H_7N_3O_2$ species and formation of CuO, respectively. Complex **7** showed an endothermic peak at 80°C with 2.23% weight loss (Calcd 2.64) due to loss of H_2O; another endothermic peak at 140°C, with 7.48% weight loss (Calcd 7.68%), from loss of hydroxide (3OH); an exothermic peak at 360°C, with 23.34% weight loss (Calcd 23.11%), corresponding to loss of $C_5H_7N_3O_2$; and an exothermic peak at 470°C, with 16.13% weight loss (Calcd 15.96%), due to formation of NiO. Complex **8** showed an endothermic peak at 80–110°C, with 9.32% weight loss (Calcd 9.8%), due to loss of $4H_2O$; exothermic peaks at 235, 340 and 470°, with 8.9, 22.58 and 16.0% weight losses (Calcd 7.6, 22.1 and 15.53%), corresponding to loss of hydroxide (3OH), $C_6H_7N_3O$ and the formation of CoO, respectively. Complex **9** showed an endothermic peak at 85°C with 12.1% weight loss (Calcd 11.69%), due to loss of $5H_2O$; another endothermic peak at 230°C, with 7.2% weight loss (Calcd 7.5%) from loss of hydroxide (3OH); an exothermic peak at 340°C with 24.1% weight loss (Calcd 24.16%), due to loss of $C_6H_6N_3O_2$; another exothermic peak at 450°C with 16.13% weight loss (Calcd 16.98%), corresponding to formation of ZnO [14, 53].

Table 4. The percent effect of the ligand **1** and metal complexes on microorganisms at different concentrations.

No. of Comp.	At 250 μg mL^{-1}	At 200 μg mL^{-1}	At 150 μg mL^{-1}
1	22	14	8
2	25	17	11
3	32	24	16
4	0	0	0
5	30	22	12
6	25	16	10
8	25	16	8
9	35	25	18
10	40	26	18

The percent effect = (diameter of zone/diameter of Petri dish) × 100; Fungi = *Aspergillus niger*; DMF was used as antimicrobial inert sol.

Complex **10** showed an endothermic peak at 75°C with 9.1% weight loss (Calcd 8.67%), due to loss of $4H_2O$; endothermic peaks at 130–175°C, with 20.66% weight loss (Calcd 20.97%), corresponding to loss of coordinated water ($6H_2O$) and coordinated hydroxide (3OH); an exothermic peak at 300°C, with 23.4% weight loss (Calcd 23.53%), due to loss of $C_5H_7N_3O_2$; and an exothermic peak at 550°, with 14.88% weight loss (Calcd 15.50%), assigned to loss of MnO [14, 50].

3.9. *Antifungal screening*

The results obtained are presented in table 4. The activity of the metal complexes increases with increase in concentration. All the metal complexes are more potent fungicides than the ligand except **4**. Hence, they may serve as vehicles for activation of the ligand as the principle cytotoxic species [72]. This enhancement in the activity can be explained on the basis of chelation theory [73, 74]. Manganese(II) complex **10** shows higher activity than the other complexes in all concentrations. The order of activity of the complexes is **10** > **9** > **3** > **5** > **2** = **6** = **8** > **1** > **4**. The variation in activity against different "microorganisms" depends either on the impermeability of the cells of the microbes or differences in ribosome's microbial cells [75].

4. Summary

Metal complexes of triaminoxime have been synthesized and characterized by elemental analyses, spectral, thermal and ESR measurements. ESR spectra of solid copper(II) complexes show a $d_{x^2-y^2}$ ground state and cobalt(II) shows a d_z^2 ground state. Manganese(II) and zinc(II) complexes show higher activity against studied "microorganisms."

References

[1] V.T. Andriole. *Int. J. Antimicrob. Agents*, **16**, 317 (2000).
[2] M. Zucolotto Chalaca, J.D. Figueroa-Villar, J.A. Ellena, E.E. Castellano. *Inorg. Chim. Acta*, **328**, 45 (2000).

[3] W. Dinku, N. Megersa, V.J.T. Raju, T. Solomon, J.A. Jonsson, N. Retta. *Bull. Chem. Soc. Ethiopia*, **17**(1), 35 (2003).
[4] B. Kebede, N. Retta, V.J.T. Raju, Y. Chebude. *Transit. Metal Chem.*, **31**, 19 (2006).
[5] A. Zharkouskaya, A. Buchholz, W. Plass. *Eur. J. Inorg. Chem.*, 4875 (2005).
[6] A.E. Ion, E.T. Spielberg, H. Gorls, W. Plass. *Inorg. Chim. Acta*, **360**, 3925 (2007).
[7] A. Zharkouskaya, H. Gorls, G. Vaughan, W. Plass. *Inorg. Chem. Commun.*, **8**, 1145 (2005).
[8] J.R.G. Mascaros, J.M. Clemente-Juan, K.R. Dunbar. *J. Chem. Soc., Dalton Trans.*, 2710 (2002).
[9] M.D. Wilson, J.M. Yau, J.H. Robinson, D.D. Wyse, B.M. Desouza. *J. Phar-Macol. Exp. Ther.*, **266**, 1454 (1993).
[10] T.W. Thomas, A.E. Underhill. *Chem. Soc. Rev.*, **1**, 99 (1972).
[11] K. Oguchi, K. Sanui, N. Ogata. *Polym. Eng. Sci.*, **30**, 449 (1990).
[12] R.C. Maurya, R. Verma, D. Sutradhar. *Synth. React. Inorg. Met-Org. Chem.*, **33**, 435 (2003).
[13] M. Kandaz, I. Yilmaz, S. Keskin, A. Koca. *Polyhedron*, **21**, 825 (2002).
[14] A.S. El-Tabl. M.Sc. Thesis, Menoufia University, Egypt (1987).
[15] S. Wesis, H. Krommer (SKW Trostberg AG. Germany) DE 83-3341645, *Chem. Abstr.*, **104**, 206730 (1986).
[16] G. Svehla. *Vogel's Textbook of Macro and Semimicro Qualitative Inorganic Analysis*, 5th Edn, p. 212, 241, 259, 265, 272, Longman Inc., New York (1979).
[17] I.M. Müller, D. Möller. *Eur. J. Inorg. Chem.*, 257 (2005).
[18] A.S. El-Tabl, F.A. El-Saied, A.N. Al-Hakimi. *Transit. Metal Chem.*, **32**, 689 (2007).
[19] H. Kantekin, U. Ocak, Y. Gok, H. Alp. *J. Coord. Chem.*, **57**, 265 (2004).
[20] E. Tas, M. Aslanoglu, A. Kilic, Z. Kara. *Transit. Metal Chem.*, **30**, 758 (2005).
[21] K.B. Gudasi, M.S. Patil, R.S. Vadavi, R.V. Shenoy, S.A. Pati1, M. Nethaji. *Transit. Metal Chem.*, **31**, 580 (2006).
[22] J.C. Soutif, L. Quator, D. Courrel, J.C. Brosse. *Macromol. Chem.*, **187**, 561 (1986).
[23] A.S. El-Tabl, R.M. Issa. *J. Coord. Chem.*, **57**, 509 (2004).
[24] L. Mishra, A. Jha, A.K. Yadaw. *Transit. Metal Chem.*, **22**, 406 (1997).
[25] A.S. El-Tabl. *Transit. Metal Chem.*, **22**, 400 (1997).
[26] E. Tas, A. Cukuroval. *J. Coord. Chem.*, **47**, 425 (1999).
[27] E. Tas, M. Ulusoy, M. Guler, I. Yilmaz. *Transit. Metal Chem.*, **29**, 180 (2004).
[28] M. El-Behery, H. El-Twigry. *Spectrochim. Acta, Part A*, **66**, 28 (2007).
[29] F. Brezina, Z. Smekal, Z. Sindelar, R. Pastorek, J. Mrozinski. *Transit. Metal Chem.*, **21**, 287 (1996).
[30] A.S. El-Tabl, K. El-Baradie, R.M. Issa. *J. Coord. Chem.*, **56**, 1113 (2003).
[31] W.H. Hegazy. *Monatsch. Chem.*, **132**, 639 (2001).
[32] K. Nakatamato. *Infrared Spectra of Inorganic and Coordination Compounds*, 2nd Edn, Wiley Inc., New York (1967).
[33] O. Pouralimardan, A.-C. Chamayou, C. Janiak, H. Hosseini-Monfared. *Inorg. Chim. Acta*, **360**, 1599 (2007).
[34] N. Raman, A. Kulandaisamy, C. Thangaraja, P. Manisankar, S. Viswanathan, C. Vedhi. *Transit. Metal Chem.*, **29**, 129 (2004).
[35] A.S. El-Tabl. *J. Chem. Res.*, **2002**, 529 (2002).
[36] A. El-Mottaleb, M. Ramadan, W. Sawodny, H.Y.F. El-Baradie, M. Gaber. *Transit. Metal Chem.*, **22**, 211 (1997).
[37] A. Cukurovali, I. Yilmaz, S. Kirbag. *Transit. Metal Chem.*, **31**, 207 (2006).
[38] J.B. Gandhi, N.D. Kulkarni. *Transit. Metal Chem.*, **26**, 96 (2001).
[39] B. Probbakar, K. Reddy, P. Lingaiat. *Indian J. Chem.*, **27A**, 217 (1988).
[40] S. Mayadevi, K.M. Yussuff. *Synth. React. Inorg. Met.-Org. Chem.*, **27**, 319 (1997).
[41] A. Cukurovali, I. Yilmaz, S. Kirbag. *Transit. Metal Chem.*, **31**, 207 (2006).
[42] S.A. Sallam. *Transit. Metal Chem.*, **31**, 46 (2006).
[43] A.Z. El-Sonbati. *Transit. Metal Chem.*, **16**, 45 (1991).
[44] A.B.P. Lever. *Inorganic Electronic Spectroscopy*, 2nd Edn, Elsevier, Amsterdam (1984).
[45] R. Atkins, G. Brewer, E. Kokot, G.M. Mokier, E. Sinn. *Inorg. Chem.*, **24**, 127 (1985).
[46] A.S. El-Tabl, S.A. El-Enein. *J. Coord. Chem.*, **57**, 281 (2004).
[47] N.K. Singh, S.B. Singh. *Transit. Metal Chem.*, **26**, 487 (2001).
[48] R.K. Parihari, R.K. Patel, R.N. Patel. *J. Chem. Soc.*, **77**, 339 (2000).
[49] S.A. Sallam, A.S. Orabi, B.A. El-Shetary, A. Lentz. *Transit. Metal Chem.*, **27**, 447 (2002).
[50] A.S. El-Tabl, T.I. Kashar. *Polish J. Chem.*, **72**, 519 (1998).
[51] A.A. Akelah, M.M. Abbasi, N.K.H. Awad. *Indian J. Chem.*, **25A**, 923 (1986).
[52] M. Kato, Y. Muto. *Coord. Chem. Rev.*, **92**, 45 (1998).
[53] B.J. Hathaway, D.E. Billing. *Coord. Chem. Rev.*, **5**, 143 (1970).
[54] A.S. El-Tabl. *Transit. Metal Chem.*, **27**, 166 (2002).
[55] A.S. El-Tabl. *Transit. Metal Chem.*, **21**, 428 (1996).
[56] I.M. Procter, B.J. Hathaway, P.N. Nicholls. *J. Chem. Soc. (A)*, 1678 (1969).
[57] S. Chandra, U. Kamar. *Spectrochim. Acta, Part A*, **61**, 219 (2005).

[58] A.S. El-Tabl. Ph.D. Thesis, Menoufia University, Egypt (1993).
[59] H.A. Kuska, M.T. Rogers, A.E. Martell. *Coordination Chemistry*, Van Nostrand Reinhold, New York (1971).
[60] A.S. El-Tabl. *Bull. Korean Chem. Soc.*, **25**, 1 (2004).
[61] B.R. McGarvery. *Transit. Metal Chem.*, **3**, 89 (1966).
[62] D. Kivelson, R. Neiman. *J. Chem. Phys.*, **35**, 149 (1961).
[63] R.K. Ray. *Inorg. Chim. Acta*, **174**, 257 (1990).
[64] J.M. Assour. *J. Chem. Phys.*, **43**, 2477 (1965).
[65] S.E. Harrison, J.M. Assour. *J. Chem. Phys.*, **41**, 365, 149 (1961).
[66] Z.W. Mao, K.B. Yu, D. Chen, S.Y. Han, Y.X. Sui, W.X. Tang. *Inorg. Chem.*, **32**, 3104 (1993).
[67] M.M. Bhadbhade, D. Srinivas. *Inorg. Chem.*, **32**, 5458 (1993).
[68] M.C.R. Symons. *Chemical and Biochemical Aspects of Electron Spin Resonance*, Van Nostrand Reinhold, Wokingham (1979).
[69] A.S. El-Tabl, R.M. Issa, M.A. Morsi. *Transit. Metal Chem.*, **29**, 543 (2004).
[70] A.S. El-Tabl, S.M. Imam. *Transit. Metal Chem.*, **22**, 259 (1997).
[71] M. Gaber, M.M. Ayad. *Thermochim. Acta*, **176**, 21 (1991).
[72] T.J. Franklin, G.A. Snow. *Biochemistry of Antimicrobial Action*, 2nd Edn, Chapman and Hall, London (1971).
[73] S.K. Sengupta, O.P. Pandey, B.K. Srivastava, V.K. Sharma, *Transit. Metal Chem.*, **23**, 349 (1998).
[74] C.H. Collins, P.M. Lyn. *Microbial Methods*, University Park Press, Baltimore (1970).
[75] M. Kurtoġlu, M.M. Dağdelen, S. Toroğlu. *Transit. Metal Chem.*, **31**, 382 (2006).